# On Robustness of Ultra-Wideband (UWB) Precoding Against Timing Jitter

Yu-Hao Chang[1], Shang-Ho Tsai[2], Xiaoli Yu[1] and C.-C. Jay Kuo[1]
Ming Hsieh Department of Electrical Engineering, University of Southern California, Los Angeles, CA, USA[1]
Department of Electrical and Control Engineering, National Chiao Tung University, Hsinchu, Taiwan[2]
E-mails: {yuhaocha,xiaoliyu}@usc.edu, shanghot@mail.nctu.edu.tw and cckuo@sipi.usc.edu

***Abstract*—The channel phase precoding (CPP) technique was recently proposed for the ultra-wideband (UWB) communication system in [1] to save the feedback overhead and the computational complexity as compared with the time-reversal prefilter (TRP) technique [2]. Two ideal assumptions have been made in both systems; namely, the availability of accurate channel information and perfect synchronization of transmitted pulses. In this work, we examine the impact of timing jitter on the performance of TRP and CPP and show that the CPP-UWB system is more robust against the timing jitter than the TRP-UWB system.**

## I. Introduction

To design receivers for ultra-wideband (UWB) communication systems, one idea [3] is to employ tens or even hundreds of rake fingers to acquire sufficient signal power along different paths. This design is however complicated and expensive. More recently, the time-reversal prefiltering (TRP) technique was proposed in [2] to concentrate the signal power so that the number of rake fingers can be significantly reduced and the design of UWB receivers can be greatly simplified. The basic idea of TRP is to use the time-reversed channel impulse response to preprocess the original transmit data so that the signal power is focused at the receiver automatically.

The TRP scheme demands the channel knowledge at the transmitter. To feedback the channel information from the receiver to the transmitter is challenging due to the large number of channel taps in an UWB channel response. The channel phase precoded UWB (CPP-UWB) transceiver design was proposed in [1] to mitigate this problem. Rather than employing the full channel information for symbol precoding, the CPP-UWB transmitter encodes the transmit data with the reversed channel phase. Please note that the UWB channel response is real since it is a baseband communication system in nature. The phase information actually corresponds to the sign of each tap, and its value can be represented by one bit. Consequently, the feedback overhead is greatly reduced. The CPP-UWB system leads to concentrated signal power at the receiver since signals transmitted along different paths are added constructively. Since not all the channel knowledge is utilized at the transmitter, the decoding performance of CPP is worse than that of TRP.

The performance of TRP-UWB and CPP-UWB schemes depends on the correct channel estimation and ideal timing synchronization. It was shown in [4] that a small amount of timing mismatch leads to great performance degradation. In this work, we study and compare the robustness of TRP-UWB and CPP-UWB systems against the timing jitter, and conclude that the CPP-UWB system is more robust than the TRP-UWB system in this measure.

The rest of the paper is organized as follows. The UWB channel model and the system block diagrams for TRP and CPP are presented in Sec. II. Then, the channel estimation scheme proposed in [1] is revisited and the timing jitter is considered in Sec. III. We analyze the performance of the two precoded systems with respect to a received pulse waveform in the presence of the time jitter in Sec. IV. Computer simulation is performed to evaluate the robustness of two precoding systems in Sec. V. Finally, concluding remarks are drawn in Sec. VI.

## II. System Models

The carrierless tap-delay-line (TDL) channel model [5] is adopted for the UWB channel modeling. It can be written as

$$h(t) = \sum_{i=0}^{L-1} h_i \delta(t - i\Delta) = \sum_{i=0}^{L-1} p_i \alpha_i \delta(t - i\Delta), \qquad (1)$$

where $h_i = p_i \alpha_i$, $L$ is the total number of signal paths, $\delta(x)$ is the Dirac delta function of $x$, $\Delta$ is the multipath resolution which is set as the time domain pulse width, $p_i \in \{+1, -1\}$ with equal probability is the $i$th phase component, and the corresponding amplitude component $\alpha_i$ is modeled as a Rayleigh random variable whose probability density function (PDF) is

$$f_{\alpha_i}(x) = \frac{x}{\sigma_i^2} e^{-x^2/2\sigma_i^2}. \qquad (2)$$

Furthermore, the power of each tap decreases exponentially with respect to its index, *i.e.,*

$$E\{\alpha_i^2\} = 2\sigma_i^2 = \Omega\gamma^i, \qquad (3)$$

where $E\{x\}$ is the expectation of random variable $x$, $\Omega$ is the power of the first tap, and $\gamma = e^{-\Delta/\Gamma}$. In the context of our interest, we assume that the channel coherent time is long enough so that the channel is invariant during the transmission of one package of data symbols.

The block diagram of a generic precoded UWB system is shown in Fig. 1, where the channel information is estimated at the receiver and then sent back to the transmitter for symbol precoding. A different amount of channel information is used in different precoding schemes. That is, the channel phase


1930-529X/07/$25.00 © 2007 IEEE

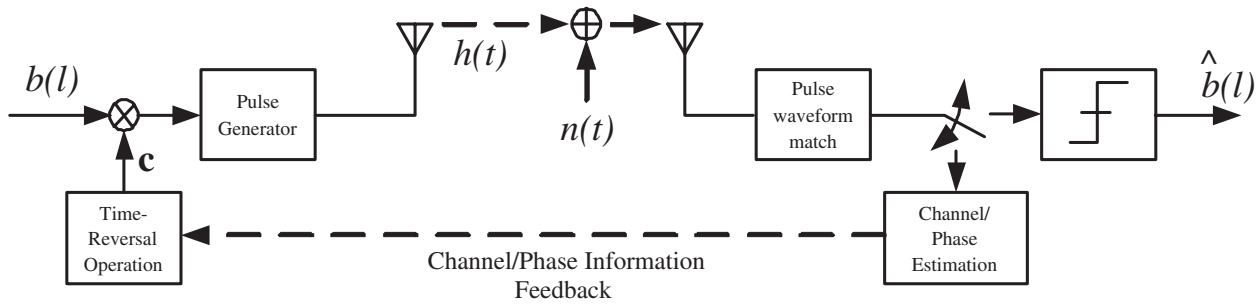


Fig. 1. The block diagram of a generic precoded UWB system.

information represented by $p_i$ in (1) is required by CPP while the complete channel knowledge that contains both $p_i$ and $\alpha_i$ is demanded by TRP. Since a different amount of channel information is fed back to the transmitter, the two precoding schemes have different complexity and performance tradeoff [1].

Let the fed back channel and phase information available for TRP and CPP be $\hat{\mathbf{h}} = [\hat{h}_0, \cdots, \hat{h}_{L-1}]^T$ and $\hat{\mathbf{p}} = [\hat{p}_0, \cdots, \hat{p}_{L-1}]^T$, respectively. The precoder reverses and normalizes the received data to form the code sequence $\mathbf{c}$ as

$$\begin{aligned}\mathbf{c} &= [c_0, \cdots, c_{L-1}]^T \\ &= \begin{cases} \frac{1}{\sqrt{L}}[\hat{p}_{L-1}, \cdots, \hat{p_0}]^T, & \text{for the CPP precoder,} \\ \frac{1}{||\hat{\mathbf{h}}||}[\hat{h}_{L-1}, \cdots, \hat{h_0}]^T, & \text{for the TRP precoder,} \end{cases}\end{aligned}$$

where $\mathbf{x}^T$ and $||\mathbf{x}||$ denote the transpose and the 2-norm of vector $\mathbf{x}$, respectively. The $l$th antipodal data symbol $b(l)$ with unit power (*i.e.,* $E\{b(l)^2\} = 1$) is encoded by $\mathbf{c}$ and then modulated by pulse waveform $w_s(t)$. As a result, the transmit signal becomes

$$x_s(t) = \sum_{l=-\infty}^{\infty} b(l) \sum_{j=0}^{L-1} c_j w_s(t - lT_s - j\Delta - \epsilon_{l,j}), \quad (4)$$

where $\epsilon_{l,j}$ is the timing jitter for the $j$th emitted chip of the $l$th data symbol and the symbol interval, $T_s = M\Delta$, is assumed to be an integer multiple of the pulse width. The timing jitter $\epsilon_{l,j}$ is modeled as an independent, identically distributed (i.i.d.) random variable with respect to $(l, j)$.

After passing through the channel and antennas at both sides, the received signal is

$$\begin{aligned} y(t) &= \sum_{l=-\infty}^{\infty} b(l) \sum_{j=0}^{L-1} \sum_{k=0}^{L-1} c_j h_k \times \\ &\quad w_r(t - lT_s - (j+k)\Delta - \tau - \epsilon_{l,j}) + n(t), \quad (5) \end{aligned}$$

where $w_r(t)$ is an unit-power received pulse waveform, $\tau$ is the propagation delay, and $n(t)$ is the zero-mean white Gaussian noise process whose two-sided power spectral density (PSD) is equal to $N_0/2$. Please note that $w_r(t)$ is usually different from $w_s(t)$ due to the antenna effect. Here, it is assumed that $w_r(t)$ is known to the receiver.

If the channel knowledge at the transmitter is perfect, (*i.e.,* $c_j = p_{L-1-j}/\sqrt{L}$ for CPP or $c_j = h_{L-1-j}/||\mathbf{h}||$ for TRP) and $\epsilon_{l,j} = 0$ for all values of $l$ and $j$, we can show from (5) that there will be a strong peak signal when indices $j$ and $k$ in (5) satisfy $j + k = L - 1$. This is resulted from the fact that all multipath components are coherently combined after certain delay. The concentrated signal power at the receiver simplifies the task of symbol decoding since the number of rake fingers required to collect a sufficient amount of power is greatly reduced.

For symbol detection, we consider a simple scheme where the receiver uses only the peak signal to determine the transmit symbol, *i.e.,* the receiver matches the peak pulse waveform and then takes a sample to estimate transmitted symbol $b(l)$. That is, after compensating propagation delay $\tau$, we can obtain the $l$th receive sample $r[l]$ as

$$r[l] = \int_{-\infty}^{\infty} y(t) w_r(t - lT_s - (L-1)\Delta - \tau) dt. \quad (6)$$

Please note that we do not examine the timing jitter effect at the receiver since it can be jointly considered in $\epsilon_{l,j}$. Finally, the $l$th data symbol can be estimated via

$$\hat{b}(l) = \text{sign}\{r[l]\}. \quad (7)$$

## III. Channel Estimation with Timing Jitter

We study the channel estimation problem in the presence of timing jitter in this section. A training-based estimation scheme was proposed in [1] to identify the phase information of the channel. However, no timing error has been considered in previous work. Given the timing jitter model in Sec. II, we need to revisit the channel estimation problem.

We modify the training-based channel estimation scheme in [1] to obtain a new estimation scheme as described below.

1) After the channel is synchronized, $N$ known channel sounding pulses, $b_T(0), \cdots, b_T(N-1)$, of a low duty cycle are emitted by the transmitter so that the received data of different transmit symbols do not overlap with each other. The emitted training signal is of the form

$$x_T(t) = \sum_{i=0}^{N-1} w_s(t - iT) b_T(i), \quad (8)$$

where $T(> L\Delta)$ is the time interval between two consecutive pulses.

2) The receiver digitizes the incoming data by performing the pulse waveform match and sampling at every $\Delta$ time


1930-529X/07/$25.00 © 2007 IEEE

instance. All $N$ discrete received signals are demodulated and then averaged to reduce noise perturbation before the channel (or phase) estimation task. Consequently, the average $k$th sample is computed as

$$r_T[k] = \frac{1}{N}\sum_{l=0}^{N-1} b_T(l) * \int_{-\infty}^{\infty} y_T(t) w_r(t - lT - k\Delta - \tau - \epsilon_{l,k})dt, \quad (9)$$

where

$$y_T(t) = \sum_{i=0}^{N-1} b_T(i) \sum_{j=0}^{L-1} h_j w_r(t - j\Delta - iT - \tau) + n(t), \quad (10)$$

and $\epsilon_{l,k}$ is the timing jitter at the $k$th channel sample of the $l$th training symbol.

3) The tap and the phase of the $k$th channel path are estimated by

$$\begin{cases} \hat{h}_k = r_T[k], \\ \hat{p}_k = \text{sign}\left\{r_T[k]\right\}. \end{cases} \quad (11)$$

It is worthwhile to mention that a one-bit analog-to-digital converter (ADC) is sufficient for the phase estimation while a high resolution ADC is needed to estimate the channel response for the tap estimation. Thus, the CPP receiver has a lower complexity than the TRP receiver.

## IV. Performance Analysis

The performance of channel estimation and symbol decoding is analyzed in this section. Since the system performance depends on the received pulse waveform, $w_r(t)$ is assumed to be a normalized, second derivative, mono-Gaussian pulse [6]. Mathematically, we have

$$w_r(t) = \frac{1}{\sqrt{E}}\bar{w}_r(t),$$

where

$$\bar{w}_r(t) = \left(1 - 4\pi\left(\frac{t}{t_n}\right)^2\right) e^{-2\pi\left(\frac{t}{t_n}\right)^2},$$

$$E = \int_{\infty}^{\infty} \bar{w}_r(t)^2 dt,$$

and $t_n$, which controls the time domain spread of the pulse waveform (*i.e.,* the pulse width), should be carefully selected so that $w_r(t) \approx 0\ \forall |t| > \Delta/2$. Also, the autocorrelation function of $w_r(t)$ is equal to [6]

$$\begin{aligned} \phi_{w_r}(\tau) &= \int_{-\infty}^{\infty} w_r(t) w_r(t-\tau) dt \\ &= \left(1 - 4\pi\left(\frac{\tau}{t_n}\right)^2 + \frac{4\pi^2}{3}\left(\frac{\tau}{t_n}\right)^4\right) e^{-\pi\left(\frac{\tau}{t_n}\right)^2}. \end{aligned}$$

An example of $\phi_{w_r}(\tau)$ with $t_n = 0.105$ ns, which corresponds to $\Delta = 240$ ps, is plotted in Fig. 2.

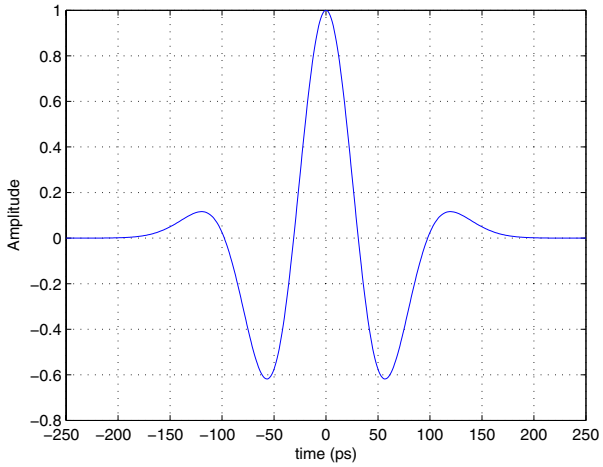


Fig. 2. The autocorrelation function $\phi_{w_r}(\tau)$ for $t_n = 105$ ps with $\Delta$=240 ps.

### A. MSE of both Channel and Phase Estimation

We first examine the performance of the proposed channel estimation scheme in a timing jitter environment. By substituting (10) in (9) and performing some manipulations, we can rewrite (9) as

$$r_T[k] = \frac{1}{N}\sum_{l=0}^{N-1}\left(b_T(l)\sum_{i=0}^{N-1} b_T(i)\times \sum_{j=0}^{L-1} h_j \phi_{w_r}(\epsilon_{l,k} + (k-j)\Delta + (l-i)T) + n_l[k]\right), \quad (12)$$

where

$$n_l[k] = b_T(l)\int_{-\infty}^{\infty} n(t) w_r(t - lT - k\Delta - \tau - \epsilon_{l,k})$$

is the corresponding noise sample, which is a white Gaussian random variable with zero-mean and variance $N_0/2$. It is denoted as

$$n_l[k] \sim \mathcal{N}(0, N_0/2). \quad (13)$$

We conclude from Fig. 2 that $\phi_{w_r}(\tau) \neq 0$ for $-0.75\Delta \leq \tau \leq 0.75\Delta$, which implies that

$$\phi_{w_r}(\epsilon_{l,k} \pm k\Delta) \approx 0 \quad \forall k \in \{\pm 1, \pm 2, \cdots\},\ \text{if } |\epsilon_{l,k}| \leq \frac{\Delta}{4}. \quad (14)$$

The condition in (14) generally holds since the value of $\epsilon_{l,k}$ is usually smaller than $\Delta$. Hence, (12) can be approximated as

$$r_T[k] \approx \frac{1}{N}\left(\sum_{l=0}^{N-1}\phi_{w_r}(\epsilon_{l,k})\right) h_k + \frac{1}{N}\sum_{l=0}^{N-1} n_l[k]. \quad (15)$$

Next, we evaluate the mean-square-error (MSE) of two estimation schemes given in (11) for a fixed channel realization. If $N$ is sufficiently large, by the Central Limit Theory [7], we can have the following approximation

$$\frac{1}{N}\left(\sum_{l=0}^{N-1}\phi_{w_r}(\epsilon_{l,k})\right) \sim \mathcal{N}(m_{\phi_{w_r}}, \frac{1}{N} Var\phi_{w_r}), \quad (16)$$


1930-529X/07/$25.00 © 2007 IEEE

and

$$\frac{1}{N}\sum_{l=0}^{N-1} n_l[k] \sim \mathcal{N}\left(0, \frac{N_0}{2N}\right), \tag{17}$$

where $m_{\phi_{w_r}} = E\{\phi_{w_r}(\epsilon_{l,k})\}$ and $Var\phi_{w_r} = E\{\phi_{w_r}(\epsilon_{l,k})^2\} - m^2_{\phi_{w_r}}$ are the mean and the variance of random variable $\phi_{w_r}(\epsilon_{l,k})$, respectively. Furthermore, for the pulse autocorrelation function considered in Fig. 2, $m_{\phi_{w_r}}$ is greater than zero since the range of jitter is usually small. The linear combination of two Gaussian random variables is still Gaussian so that $r_T[k]$ has the following distribution

$$r_T[k] \sim \mathcal{N}\left(h_k m_{\phi_{w_r}}, \frac{h_k^2}{N} Var\phi_{w_r} + \frac{N_0}{2N}\right). \tag{18}$$

Hence, the probability of the phase estimation error on the $k$th phase component is evaluated as

$$\begin{aligned} Pe_k &= Pr\{p_k \neq \hat{p}_k\} = Pr\{r_T[k] < 0 \big| p_k = 1\} \\ &= Q\left(\frac{\alpha_k m_{\phi_{w_r}}}{\sqrt{\frac{h_k^2}{N} Var\phi_{w_r} + \frac{N_0}{2N}}}\right), \end{aligned} \tag{19}$$

where $Q(x)$ is defined as

$$Q(x) = \int_x^\infty \frac{1}{\sqrt{2\pi}} e^{-x^2/2} dt. \tag{20}$$

Conditioned on one fixed channel realization $\mathbf{h}$, the MSE of the phase estimation becomes

$$\begin{aligned} \mathrm{MSE}_{\mathbf{p}} &= \sum_{k=0}^{L-1} E\{|p_k - \hat{p}_k|^2 \big| \mathbf{h}\} \\ &= \sum_{k=0}^{L-1} Pr\{p_k \neq \hat{p}_k\}(p_k - \hat{p}_k)^2 = \sum_{k=0}^{L-1} 4Pe_k. \end{aligned} \tag{21}$$

It is worthwhile to point out that the error probability $Pe_k$ in (19) goes to zero asymptotically as $N$ goes up. Therefore, we know from (21) that the phase estimation error could be very small as long as $N$ is large enough.

On the other hand, the MSE of the proposed channel estimation scheme in (11) is

$$\mathrm{MSE}_{\mathbf{h}} = \sum_{k=0}^{L-1} E\{|h_k - \hat{h}_k|^2 \big| \mathbf{h}\} = \sum_{k=0}^{L-1} E\{|h_k - r_T[k]|^2 \big| \mathbf{h}\}. \tag{22}$$

By substituting (15) into (22) and performing some manipulations, we have

$$\mathrm{MSE}_{\mathbf{h}} = \sum_{k=0}^{L-1} \left(\alpha_k^2 (1 - m_{\phi_{w_r}})^2 + \frac{1}{N} Var_{\phi_{w_r}} + \frac{N_0}{2N}\right). \tag{23}$$

Therefore, we have

$$\lim_{N\to\infty} \mathrm{MSE}_{\mathbf{h}} = \sum_{i=0}^{L-1} \alpha_i^2 (1 - m_{\phi_{w_r}})^2 \geq 0, \tag{24}$$

as long as $m_{\phi_{w_r}} \neq 1$. As compared with $\mathrm{MSE}_{\mathbf{p}}$, $\mathrm{MSE}_{\mathbf{h}}$ could not be arbitrarily small even if $N$ goes to infinity.

### *B. Output SNR for CPP-UWB Systems*

A similar approach can be used to analyze the output signal-to-noise ratio (SNR) of CPP at $r[l]$ when timing jitters exist. Here, due to the space limitation, we consider the ISI-free case only, *i.e.,* $T_s > L\Delta$. In addition, the phase information available for symbol precoding is assumed to be ideal in order to simplify the analysis. After some manipulations, the discrete sample for the $l$th transmit data from the CPP transmitter can be expressed as

$$r[l] = b(l) \sum_{k=0}^{L-1} \frac{p_k}{\sqrt{L}} h_k \phi_{w_r}(\epsilon_{l,L-1-k}) + n[l], \tag{25}$$

where

$$\begin{aligned} n[l] &= \int_{-\infty}^{\infty} n(t) w_r(t - lT_s - (L-1)\Delta - \tau) dt \\ &\sim \mathcal{N}(0, N_0/2) \end{aligned}$$

is the corresponding noise sample. The output SNR for CPP is calculated as

$$SNR_{CPP} = \frac{E\left\{\left(\frac{1}{\sqrt{L}} \sum_{k=0}^{L-1} \alpha_k \phi_{w_r}(\epsilon_{l,L-1-k}) b(l)\right)^2\right\}}{E\{|n[l]|^2\}}.$$

With some mathematical manipulations, we have

$$\begin{aligned} SNR_{CPP} = &\frac{\pi\Omega}{2LN_0} \left(\frac{1-\gamma^{L/2}}{1-\gamma^{1/2}}\right)^2 m^2_{\phi_{w_r}} + \\ &\frac{2\Omega}{LN_0} \frac{1-\gamma^L}{1-\gamma} \left(Var_{\phi_{w_r}} + \left(1 - \frac{\pi}{4}\right) m^2_{\phi_{w_r}}\right). \end{aligned} \tag{26}$$

If the values of $m_{\phi_{w_r}}$ and $Var_{\phi_{w_r}}$ are fixed while the pulse width approaches infinitesimal, *i.e.,* $\Delta \to 0$ ($\gamma \to 1$), the second term at the right-hand side of (26) becomes much smaller than the first term at the same side. As a result, we can get

$$\lim_{\Delta\to 0} SNR_{CPP} \approx \frac{\pi\Omega}{2LN_0} \left(\frac{1-\gamma^{L/2}}{1-\gamma^{1/2}}\right)^2 m^2_{\phi_{w_r}}. \tag{27}$$

It is clear that the output SNR for the CPP system degrades as a factor of $m^2_{\phi_{w_r}}$ as compared with the same system without timing jitter. Please note that the above result is derived under the assumption that the ideal phase information is available for symbol precoding. The output SNR given in (27) can be treated as an upper bound for realistic systems using the estimated channel phase for precoding. The gap becomes tight when the noise power reduces as studied in the next section.

## V. Simulation Results

Computer simulation is conducted to evaluate the performance of TRP and CPP in a timing jitter environment. The system parameters are: $\Delta = 240$ ps ($t_n = 0.105$ ns), $\Gamma = 7.5$ ns (CM1) and $L = 140$. The timing jitter $\epsilon_{l,j}$ is modeled as a truncated normal random variable whose range is limited within $[-\Delta/4, +\Delta/4]$. The corresponding PDF for $\epsilon_{l,j}$ is given by

$$f_{\epsilon_{l,j}}(x) = \frac{1}{M} e^{-x^2/2\sigma^2}, \tag{28}$$


1930-529X/07/$25.00 © 2007 IEEE

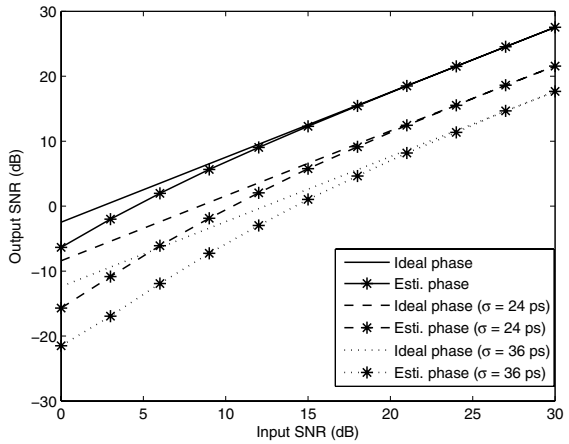


Fig. 3. Comparison of the output SNR as a function of the input SNR value with different timing jitter power.

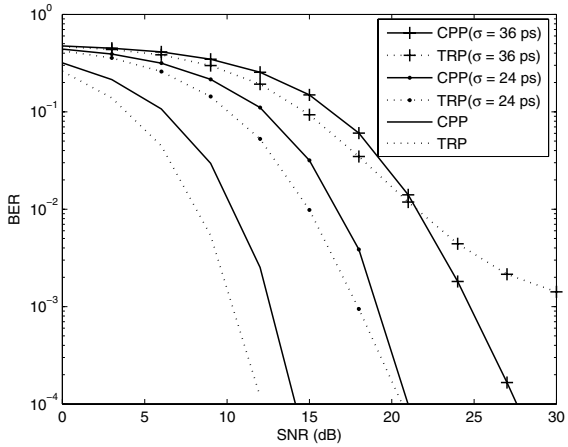


Fig. 4. Comparison of the BER performance curves as a function of the SNR value with different timing jitter power.

where

$$M = \int_{-\Delta/4}^{-\Delta/4} e^{-x^2/2\sigma^2} dx \tag{29}$$

is a constant used to normalize the PDF function and $\sigma$ that controls the jitter power will be specified later. Simulation results reported here are obtained as the average of 1000 independent channel realizations.

First, we compare the output SNR of CPP-UWB systems using imperfect phase information for symbol precoding under different jitter power. Here, 100 training symbols are used to extract the channel phase information. To simulate different jitter power, we choose $\sigma$ to be 24 and 36 ps, respectively. The SNR curves derived in (27), are plotted for performance benchmarking. The output SNR as a function of the input SNR value is plotted in Fig. 3. If the phase knowledge at the transmitter is flawless and timing at both ends of the link is perfect, there will be an approximately 3 dB loss at the output SNR due to the partial channel information is utilized for precoding [8]. Although the imperfect phase knowledge introduces performance degradation, the gap does shrink as SNR goes up for all jitter environments since the error power in the phase estimation process becomes smaller. Moreover, when the phase information is ideal, the performance loss caused by different jitter power, namely, $\sigma = 24$ and 36 ps, are 5.95 and 9.92 dB, respectively. This observation confirms our theoretical results provided in (27).

Next, we simulate the decoding performance for both TRP and CPP systems in the presence of timing jitter. Again, we apply 100 training symbols to acquire either the channel or phase information and keep all other system parameters unchanged. The simulation results are shown in Fig. 4, where the performance curves for both ideal CPP and TRP systems without timing jitters are plotted for the reference purpose. As shown in Fig. 4, the ideal performance of CPP is worse than that of TRP since only partial channel information is employed in the precoding process. The performance of both precoding systems degrades as the timing jitter exists. The performance gap between TRP and CPP reduces as the jitter power increases. If we keep increasing the jitter power, *e.g.*, $\sigma = 36$ ps, it is interesting to see that CPP even outperforms TRP when SNR is greater than 22 dB. This can be explained as follows. A stronger timing jitter also leads to a larger SNR variation in TRP than CPP. This is especially true when the noise power is weak. Since BER is very sensitive to SNR, the averaged decoding performance of TRP is worse. Therefore, we conclude that the BER performance of TRP is more sensitive to the timing error than that of CPP.

## VI. Conclusion and Future Work

The performance of two UWB precoding methods, TRP and CPP, in the presence of timing jitter was compared in this work. It was shown that CPP provides a more robust BER performance than TRP against the timing jitter when the jitter becomes more significant. Our current study is still preliminary. A more thorough comparison is being conducted and will be reported in the near future.

## References

[1] Y.-H. Chang, S.-H. Tsai, X. Yu, and C.-C. J. Kuo, "Design and analysis of channel-phase-precoded ultra wideband (CPPUWB) systems," in *Proc. IEEE WCNC'06*, Apr. 2006.

[2] T. Strohmer, M. Emami, J. Hansen, G. Papanicolaous, and A. J. Paulraj, "Application of time-reversal with MMSE equalization to UWB communications," in *Proc. IEEE GLOBECOM'04*, Nov. 2004.

[3] M. Z. Win and R. A. Scholtz, "On the energy capture of ultrawide bandwidth signals in dense multipath environments," *IEEE Communications Letters*, vol. 2, no. 9, pp. 245–247, Sep. 1998.

[4] W. M. Lovelace and J. K. Townsend, "The effects of timing jitter and tracking on the performance of impulse radio," *IEEE Journal on Selected Areas in Communications*, vol. 20, no. 9, pp. 1646–1651, Dec. 2002.

[5] Y.-L. Chao and R. A. Scholtz, "Ultra-wideband transmitted reference systems," *IEEE Trans. on Vehicular Technology*, vol. 54, no. 5, pp. 1556–1569, Sep. 2005.

[6] F. Ramirez-Mireles and R. A. Scholtz, "Multiple-access performance limits with time hopping and pulse position modulation," in *Proc. IEEE MILCOM'98*, Oct. 1998.

[7] A. Papoulis, *Probability, Random Variables, and Stochastic Processes*, 3rd ed. McGraw-Hill, 1991.

[8] Y.-H. Chang, S.-H. Tsai, X. Yu, and C.-C. J. Kuo, "Ultra-wideband (UWB) transceiver design using channel phase precoding (CPP)," *to appeare in IEEE Trans. on Signal Processing*, (See also http://viola.usc.edu/People/people.jsp?uid=fuzzyfr).